JOURNAL OF AIRCRAFT
Vol. 31, No. 5, Sept.–Oct. 1994

Waveriders with Finlets

X. He,* M. L. Rasmussen,† and R. A. Cox‡
University of Oklahoma, Norman, Oklahoma 73019

A generalized analytical method for designing waverider shapes is presented. Waverider configurations that incorporate finlets are of primary interest. These finlets resemble fins on conventional aircraft and might imaginably be used as control surfaces. The design methodology determines the waverider shape by alternatively specifying the planform shape, the freestream-surface trailing-edge shape, the compression-surface trailing-edge shape, or various combinations of the three. A wide variety of shapes is presented, and the aerodynamic properties are calculated by means of hypersonic small-disturbance theory. The effects of finlets are to shift the c.p. aft and to improve static stability. The results are novel, and the analysis is readily usable for a variety of design studies.

Nomenclature

A, B, C, D = coefficients for planform curve
b = width of waverider in the base plane
C_D = drag coefficient
C_f = average skin friction coefficient
C_L = lift coefficient
D_f = friction drag
D_w = wave drag
K_δ = hypersonic similarity parameter, $\equiv M_\infty \delta$
L/D = lift-to-drag ratio
l = length of basic cone
l_w = length of waverider
M_∞ = freestream Mach number
q_∞ = freestream dynamic pressure
$R_{\infty b}$ = normalized radial distance to freestream surface in the base plane
R_{cb} = normalized radial distance to compression surface in the base plane
Re_{lw} = Reynolds number based on the waverider length
R_0 = normalized radial distance to freestream surface in symmetry plane
r = radial distance from the vertex of the basic cone
S_p = projected planform area
S_w = wetted surface area
V = volume of waverider
$V^{2/3}/S_p$ = volumetric ratio
X, Y, Z = normalized Cartesian coordinates
X_σ, Y_σ = normalized shock location in the base plane
z^*_{cp} = center of pressure as a percent of waverider length
z^*_{cv} = center of volume as a percent of waverider length
β = shock angle
γ = ratio of specific heats
Δz_{sm} = static margin as a percent of waverider length
δ = half-cone angle
θ = polar angle measured from the z axis
σ = ratio of shock angle to cone angle
ϕ = azimuthal angle measured from the x axis
ϕ_l = anhedral angle

Presented as Paper 93-3442 at the AIAA Applied Aerodynamics Conference, Monterey, CA, Aug. 9–11, 1993; received Sept. 26, 1993; revision received Jan. 29, 1994; accepted for publication Jan. 29, 1994.

*Adjunct Assistant Professor, School of Aerospace and Mechanical Engineering, 865 Asp Ave. Member AIAA.
†Professor, School of Aerospace and Mechanical Engineering, 865 Asp Ave. Associate Fellow AIAA.
‡Assistant Professor, School of Aerospace and Mechanical Engineering, 865 Asp Ave. Member AIAA.

Introduction

THE waverider concept has been around for some time, starting first with the two-dimensional-flow caret configurations of Nonweiler,[1] and the axisymmetric cone-flow configurations of Jones.[2] More recently, waveriders derived from nonaxisymmetric conical flows have been studied by Rasmussen.[3] The waverider concept came from early re-entry vehicle design, and remained only of theoretical interest until the design of a transatmospheric and aerospace vehicle became of interest. The National Aero-Space Plane (NASP) brought renewed interest in the waverider concept and recently led to an international symposium.

Waverider-based vehicles are of interest because they provide a large L/D. For waveriders to be incorporated into practical aircraft designs, they must be enhanced with control surfaces of various sorts, propulsion units, and other configurational additions. After all the additions and alterations have been made, the resulting overall configurations may altogether cease to be waveriders. Aside from whether or not this is desirable, it is of interest to know what alterations can be made that still retain the waverider feature. In this regard, there are a great variety of waverider shapes that have not been explored, and, in fact, are not commonly known. Some of these involve blended winglets, fins, and cowlings that are part of coherent waverider shaping, and which conceivably could be used for control surfaces or cowlings for air-breathing engines. In this article, waverider shapes are developed that incorporate what are called finlets as a part of the waverider design concept. These finlets, which resemble fins on conventional aircraft, might imaginably be used as control surfaces.

Allied with this design goal, a systematic means for constructing waverider shapes is proposed that specifies forms in the planform view, or alternatively in the baseplane view, or by a combination of the two. The design approach will make use of hypersonic small-disturbance theory (HSDT), as has been previously laid out.[4–6] Using the planform view as a starting description is a new approach, and the connection with the baseplane view provides a useful interaction besides furnishing a means for evaluating the aerodynamic properties of the waverider. A variety of examples will be shown that demonstrate the broad scope of waverider shapes that can be realized.

Formulation

Consider steady inviscid supersonic flow of a perfect gas past a circular cone at zero incidence with the freestream and at Mach number M_∞. The coordinate system and nomenclature are shown in Fig. 1, and the waverider and its flowfield are described by HSDT. The methodology follows that of Rasmussen and He.[5] The shock angle β is related to the basic-cone angle δ by means of the relation

$$\sigma \equiv \frac{\beta}{\delta} = \left[\frac{\gamma + 1}{2} + \frac{1}{K_\delta^2}\right]^{1/2} \tag{1}$$

where $K_\delta \equiv M_\infty \delta$ is the hypersonic similarity parameter. For convenience, both spherical polar coordinates (r, θ, ϕ) and rectangular Cartesian coordinates (x, y, z) are used to describe the waverider surfaces, and the normalized coordinates $X \equiv x/l\delta$, $Y \equiv y/l\delta$, and $Z = z/l$ are introduced. In the rectangular Cartesian coordinates, the conic shock surface is described by

$$Z^2 = (1/\sigma^2)(X^2 + Y^2) \tag{2}$$

The leading-edge curve in the planform plane can be given by the intersection of the cone surface and a cylinder aligned with the z axis of symmetry for the basic cone. This cylinder is described by specifying Z as a function of Y

$$Z = f(Y) \tag{3}$$

as shown in Fig. 2. Equation (3) describes the freestream-surface leading-edge curve in the planform plane. The freestream-surface trailing-edge curve in the base plane can be determined by substituting Eq. (3) into Eq. (2), which yields

$$X = [\sigma^2 f^2(Y) - Y^2]^{1/2} = F(Y) \tag{4}$$

Alternatively, if the freestream trailing-edge curve is specified by $F(Y)$, then the planform function $f(Y)$ can be determined accordingly.

In the spherical polar coordinates (r, θ, ϕ), the freestream surface is described for small angles θ by

$$r = (\beta/\theta) r_s(\phi) \tag{5}$$

where $r_s(\phi)$ is the leading-edge line drawn on the conical shock $\theta = \beta$. The compression surface in the shock layer is described by

$$r = r_s(\phi)\sqrt{(\beta^2 - \delta^2/\theta^2 - \delta^2)} \tag{6}$$

The freestream and compression surfaces can thus be determined when $r_s(\phi)$ is known.

The function $r_s(\phi)$ can be specified by defining the trailing-edge of the freestream surface in the base plane. This is done by setting $r = l$ in Eq. (5); then we set $\theta = \theta_{\infty b}$:

$$\theta_{\infty b} = \beta[r_s(\phi)/l] \tag{7}$$

In the base plane, we now define a nondimensional radial distance measured from the Z axis to the freestream-surface trailing edge by $R_{\infty b} \equiv \theta_{\infty b}(\phi)/\delta$, such that

$$\begin{aligned} X &\equiv R_{\infty b} \cos \phi \\ Y &\equiv R_{\infty b} \sin \phi, \quad \text{and} \quad R_{\infty b} = [X^2 + Y^2]^{1/2} \end{aligned} \tag{8}$$

where the subscript ∞ refers to the freestream surface, and the subscript b refers to the base plane. Equation (7) now becomes

$$R_{\infty b}(\phi) = \sigma[r_s(\phi)/l] \tag{9}$$

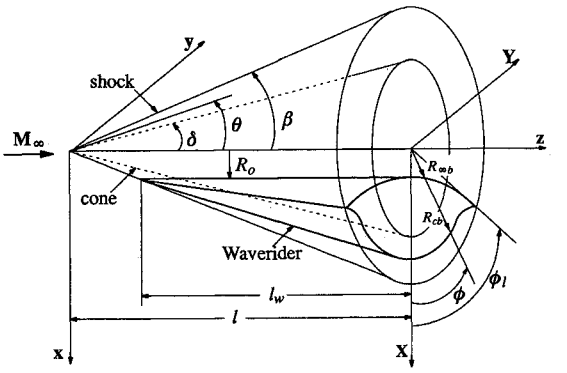

Fig. 1 Construction of a general cone-derived waverider.

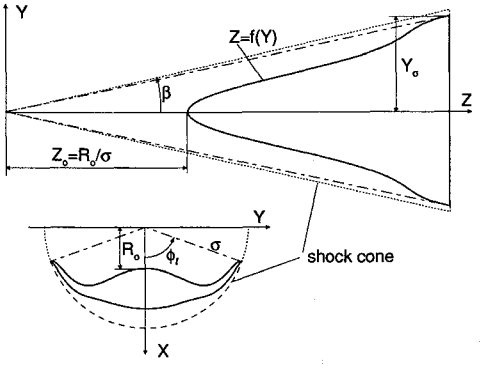

Fig. 2 Planform and base-plane description of a general cone-derived waverider.

Thus, $R_{\infty b} = \sigma$ at the shock where $\phi = \phi_l$. Let the dimensionless radial distance to the compression surface be denoted by $R_{cb} \equiv \theta_{cb}(\phi)/\delta$. Then, from Eq. (6) evaluated in the base plane, we obtain

$$R_{cb}^2(\phi) = 1 + [(\sigma^2 - 1)/\sigma^2] R_{\infty b}^2(\phi) \tag{10}$$

It is convenient to use $R_{\infty b}(0) = X(0) \equiv R_0$ as a parameter. The parameter R_0 can be interpreted geometrically as the distance down to the freestream surface from the basic-cone axis, measured in the plane of symmetry, i.e., when $\phi = 0$ or $Y = 0$ (see Fig. 2). The relation between R_0 and $Z_0 = f(0)$ is then given by

$$Z_0 \equiv (R_0/\sigma) \tag{11}$$

The length l_w of the waverider is given by

$$(l_w/l) = 1 - (R_0/\sigma) \tag{12}$$

When Eq. (3) is specified, the freestream-surface trailing-edge curve $R_{\infty b}$ is determined through Eqs. (4) and (8). The compression-surface trailing-edge curve is determined through Eq. (10). The leading-edge curve on the shock cone $r_s(\phi)$ is determined from Eq. (9), and the entire freestream and compression surfaces are determined from Eqs. (5) and (6). In general, the waverider shape can be specified by any of the planform, freestream trailing-edge, or compression trailing-edge curves separately, or in combination.

Hypersonic Small-Disturbance Analysis

The integration of the pressure force over a waverider configuration is not simple if it is carried out directly on the compression surface. The complexity is caused by the nature of the compression surface, which is a curved three-dimensional nonconical stream surface. This complexity is avoided by selecting a control surface for which the integration of the pressure force is nonzero only in the base plane.[5] When the

hypersonic small-disturbance approximations are used, the lift and wave drag are determined by quadratures involving only the freestream-surface trailing-edge curve.[5-7]

The moment acting on a body can be determined similarly, and the static margin Δz_{sm} is defined as

$$\Delta z_{sm} \equiv [(z^*_{cp} - z^*_{cv})/l_w] \tag{13}$$

where z^*_{cp} and z^*_{cv} are the center of pressure and the center of volume as a percent of the length of the waverider.[4,7] For a slender cone it can be shown that $\Delta z_{sm} = -0.083$. The static margin of a slender cone is negative since the c.p. is located ahead of the center of volume, or c.g. for a homogeneous body. Therefore, a homogeneous slender cone is statically unstable. For cone-derived waveriders without finlets, the static margin Δz_{sm} is usually more negative.[5]

The geometric properties, such as volume and wetted surface area, can also be integrated in terms of the freestream or compression functions in the base plane. The volume of the waverider is denoted by V, the planform area by S_p, and the overall wetted surface area by S_w. These geometric properties of waverider shapes can be determined by functionals involving the freestream-surface trailing-edge curve.[5-7] The aspect ratio b/l_w is given by

$$\frac{b}{l_w} = \frac{2\delta\sigma^2 \sin\phi_l}{\sigma - R_0} \tag{14}$$

and the volumetric ratio, defined as $V^{2/3}/S_p$, is used as a comparative figure of merit for the volume. The background discussion on the integral expressions for the aerodynamic and geometric properties can be found in Refs. 4–7.

The friction drag used is defined in a form that is analogous to the other components of force

$$D_f = q_\infty C_f S_w \tag{15}$$

where q_∞ is given by $q_\infty = \rho_\infty V_\infty^2/2$. Since the pressure is constant on the freestream surface and changes little on the compression surface, we assume that the local skin friction coefficients can be modeled using a flat-plate analysis along a streamline on the freestream surface and an analogous wedge analysis for the compression surface. The external-flow conditions are the freestream conditions and the downstream shock conditions, respectively. A zero-pressure gradient is assumed and crossflow in the boundary layer is ignored. We also assume that the Prandtl number is unity and the viscosity is proportional to the temperature. Although more realistic formulas can be used to estimate the average skin friction coefficient, we find that this approximate formula is sufficient for our purposes.[5]

The hypersonic small-disturbance formulation can now be used to investigate the waverider shapes generated at the on-design condition. To fix ideas, we assume a body 20 m in length, traveling at an altitude of 24 km. The freestream Reynolds number is approximately 1.55×10^8 for a freestream Mach number of 8. The value of L/D for a waverider configuration is determined as

$$\frac{L}{D} = \frac{L}{D_w + D_f} = \frac{C_L}{C_D + (S_w/S_p)C_f} \tag{16}$$

where $D_w = q_\infty C_D S_p$ and $L = q_\infty C_L S_p$. The pressure coefficient on the base is arbitrarily set at zero.

Configurations

Common Considerations

Consider several classes of waverider shapes generated by specification of the planform curves whose functional forms are given by Eq. (3). There are several conditions that must be met by these functional forms. One is that the shock occurs at $Y = Y_\sigma$, and thus that $Z(Y_\sigma) = 1$. In Cartesian coordinates the shock occurs at $X_\sigma \equiv \sigma \cos\phi_l$ and $Y_\sigma \equiv \sigma \sin\phi_l$ in the base plane. Another condition is that, in the base plane, $R_{\infty b}(\phi)$ should be single-valued in the range $0 < \phi < \phi_l$. In the planform plane, the equivalent condition is given by

$$\frac{dZ}{dY} < \frac{Z}{Y}, \qquad 0 < Y < Y_\sigma \tag{17}$$

There are other conditions at our disposal for generating various shapes of interest. The condition that $dR_{\infty b}/d\phi = 0$ at $\phi = 0$ (or $dX/dY = 0$ at $Y = 0$) in the base plane gives a freestream surface without a sharp ridge on the symmetry plane. In the planform plane, this condition is given by $dZ/dY = 0$ at $Z = Z_0$. If this condition is not satisfied, a ridge will occur on the freestream surface, a corresponding crease will occur on the compression surface, and the nose in the planform view will be pointed.

To generate a waverider with finlets with a single smooth curve in either the base plane or the planform plane, two inflection points on the curve are needed in the range of $0 < Y < Y_\sigma$. A function with nonconstant third-order derivatives is thus required for the curve. The finlets can also be generated by piecewise functions with lower-order derivatives, but the corresponding freestream and compression surfaces are no longer smooth surfaces. A ridge will occur whenever there is a slope discontinuity on the freestream-surface leading-edge curve in the planform plane.

The waverider configurations used in this work are all designed at $M_\infty = 8$ and $\delta = 10$ deg. Although varying M_∞ and δ will change the shape of the finlets, they are not the main factors for our purposes. The aerodynamic and geometric properties of these waveriders are listed in Table 1, where the first two rows are input, the next three rows show geometric output, and the last five rows contain lift, drag, and stability values.

Table 1 Properties of HSDT waveriders

Configurations	C1	C2	C3	C4	C5	C6	C7	C8	C9	C10
R_0/X_σ	0.5	0.5	0.5	1.5	2.0	2.0	1.5	0.56	0.42	0.94
ϕ_l	70 deg	70 deg	70 deg	80 deg	80 deg	80 deg	80 deg	55 deg	40 deg	50 deg
$V^{2/3}/S_p$	0.217	0.213	0.209	0.195	0.215	0.200	0.207	0.213	0.232	0.175
b/l_w	0.518	0.518	0.518	0.608	0.689	0.689	0.608	0.552	0.433	0.504
S_w/S_p	2.138	2.661	2.676	2.503	2.802	2.190	2.417	2.507	2.688	2.152
$\Delta Z_{sm} \times 10$	−0.878	−0.583	−0.576	−0.565	−0.822	−0.857	−0.713	−0.714	−0.754	−0.405
$C_L \times 10$	0.679	0.671	0.669	0.663	0.668	0.668	0.671	0.664	0.668	0.643
$C_f \times 10^3$	0.205	0.217	0.217	0.226	0.194	0.217	0.223	0.211	0.204	0.285
$C_D \times 10^2$	1.139	1.052	1.072	1.075	1.111	1.099	1.112	0.994	0.986	0.971
L/D	5.955	6.376	6.242	6.165	6.010	6.081	6.029	6.679	6.781	6.623

Piecewise Straight-Line Planform View

It is interesting to know how a waverider looks in perspective if the planform view is a delta shape. This can be done by specifying the planform curve as a single straight line

$$Z = A + BY, \qquad 0 \le Y \le Y_\sigma$$
$$A = Z_0 = R_0/\sigma \tag{18}$$
$$B = (1 - R_0/\sigma)/Y_\sigma$$

When $R_0 = 0$, the waverider shapes become idealized, for which two infinitesimally thin delta winglets are formed from planes that pass through the z axis of the basic cone. The orientation of the winglets is described by ϕ_l. When R_0 is not equal to zero, the freestream surface is curved, and the leading-edge angle is nonzero. A waverider shape with a delta planform view described by $R_0 = 0.5X_\sigma$ and $\phi_l = 70$ deg is displayed in Fig. 3. This configuration (labeled C1) is statically more unstable than a slender cone since its ΔZ_{sm} is more negative.

Consider now constructing finlets, or winglets, near the rear of the body. The single straight line in the planform plane can be replaced by two straight line segments connected at (Y_1, Z_1):

$$Z = A_1 + B_1Y, \qquad 0 \le Y \le Y_1$$
$$Z = A_2 + B_2Y, \qquad Y_1 \le Y \le Y_\sigma$$
$$A_1 = R_0/\sigma$$
$$B_1 = \frac{\omega_z}{\omega_y}\left(1 - \frac{R_0}{\sigma}\right)\frac{1}{Y_\sigma} \tag{19}$$
$$A_2 = 1 - \frac{(\sigma - R_0)(1 - \omega_z)}{\sigma(1 - \omega_y)}$$
$$B_2 = \frac{(\sigma - R_0)(1 - \omega_z)}{\sigma(1 - \omega_y)}\frac{1}{Y_\sigma}$$

where $\omega_z = (Z_1 - Z_0)/(1 - Z_0)$ and $\omega_y = Y_1/Y_\sigma$. To prevent the crossover of the freestream and compression surfaces in the base plane, ω_z and ω_y must satisfy the following condition:

$$(\omega_y/\omega_z) < 1$$

Figure 4 shows the waverider shape with a sharp finlet near the base plane in the planform view when $\omega_z = 0.7$, $\omega_y = 0.4$, $R_0 = 0.5X_\sigma$, and $\phi_l = 70$ deg. When the planform is delta-shaped, the finlets in the base plane and side views are curved and reflexed upward. The volumetric ratio remains almost the same while L/D and the static margin are both improved. This configuration is labeled C2.

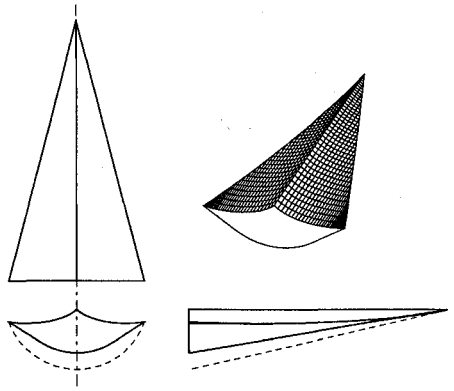

Fig. 3 C1: waverider with a delta-shaped planform for $\phi_l = 70$ deg and $R_0 = 0.5X_\sigma$.

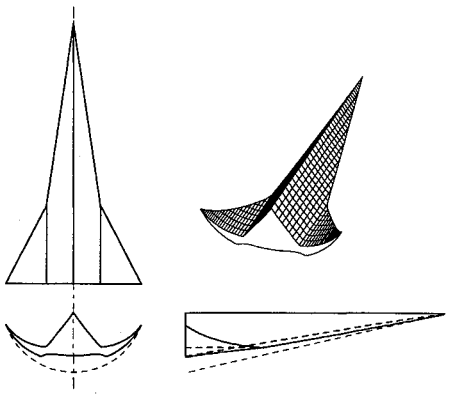

Fig. 4 C2: waverider with delta-shaped finlets for $\phi_l = 70$ deg, $R_0 = 0.5X_\sigma$, $\omega_y = 0.4$, and $\omega_z = 0.7$.

For a waverider with quadrilateral finlets, the planform of the waverider shape has to be made of at least three straight lines. We thus define three planform lines connected at two locations (Y_1, Z_1) and (Y_2, Z_2). Equation (3) now becomes

$$Z = A_1 + B_1Y, \qquad 0 \le Y \le Y_1$$
$$Z = A_2 + B_2Y, \qquad Y_1 \le Y \le Y_2$$
$$Z = A_3 + B_3Y, \qquad Y_2 \le Y \le Y_\sigma$$
$$A_1 = \frac{R_0}{\sigma}$$
$$B_1 = \frac{\omega_{z1}}{\omega_{y1}}\left(1 - \frac{R_0}{\sigma}\right)\frac{1}{Y_\sigma}$$
$$A_2 = \left(1 - \frac{R_0}{\sigma}\right)\left(\frac{\omega_{z1}\omega_{y2} - \omega_{z2}\omega_{y1}}{\omega_{y2} - \omega_{y1}}\right) + \frac{R_0}{\sigma} \tag{20}$$
$$B_2 = \frac{(\sigma - R_0)(\omega_{z2} - \omega_{z1})}{\sigma(\omega_{y2} - \omega_{y1})}\frac{1}{Y_\sigma}$$
$$A_3 = 1 - \frac{(\sigma - R_0)(1 - \omega_{z2})}{\sigma(1 - \omega_{y2})}$$
$$B_3 = \frac{(\sigma - R_0)(1 - \omega_{z2})}{\sigma(1 - \omega_{y2})}\frac{1}{Y_\sigma}$$

where $\omega_{z1} = (Z_1 - Z_0)/(1 - Z_0)$, $\omega_{z2} = (Z_2 - Z_0)/(1 - Z_0)$, $\omega_{y1} = Y_1/Y_\sigma$, and $\omega_{y2} = Y_2/Y_\sigma$. To prevent the crossover of the freestream and compression surfaces in the base plane, ω_{z1}, ω_{z2}, ω_{y1}, and ω_{y2} must satisfy the following condition:

$$(\omega_{y1}/\omega_{z1}) < (\omega_{y2}/\omega_{z2}) < 1$$

The waverider shape C3 with quadrilateral finlets near the base plane in the planform view when $\omega_{z1} = 0.7$, $\omega_{z2} = 0.8$, $\omega_{y1} = 0.4$, and $\omega_{y2} = 0.7$ for $R_0 = 0.5X_\sigma$ and $\phi_l = 70$ deg is displayed in Fig. 5. By changing the parameters R_0 and ϕ_l, the size and orientation of the finlets can be changed. Figure 6 shows the waverider shape C4 when $\omega_{z1} = 0.7$, $\omega_{z2} = 0.8$, $\omega_{y1} = 0.4$, and $\omega_{y2} = 0.7$ for $R_0 = 1.5X_\sigma$ and $\phi_l = 80$ deg. Increasing R_0 and ϕ_l at the same time will increase the size of the finlets. The side view in Fig. 6 shows that the finlets near the base plane are raised above the symmetry line on the top surface.

To prevent a ridge from being formed on the upper surface of the waverider, the straight line is replaced by a curve with $dZ/dY = 0$ at the nose in the planform plane, which produces

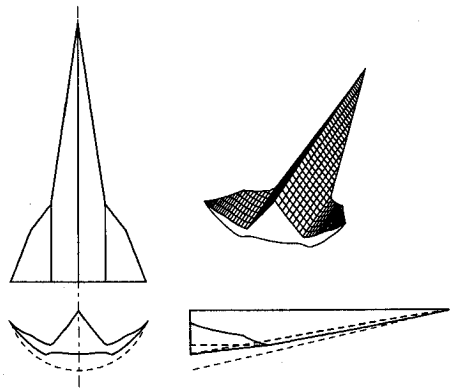

Fig. 5 C3: waverider with quadrilateral finlets for ϕ_l = 70 deg, $R_0 = 0.5X_\sigma$, $\omega_{y1} = 0.4$, $\omega_{y2} = 0.7$, $\omega_{z1} = 0.7$, and $\omega_{z2} = 0.8$.

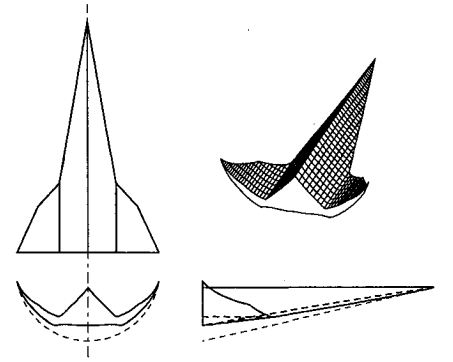

Fig. 6 C4: waverider with quadrilateral finlets for ϕ_l = 80 deg, $R_0 = 1.5X_\sigma$, $\omega_{y1} = 0.4$, $\omega_{y2} = 0.7$, $\omega_{z1} = 0.7$, and $\omega_{z2} = 0.8$.

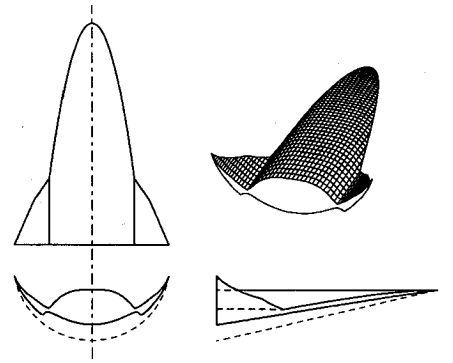

Fig. 7 C5: waverider with a rounded nose and quadrilateral finlets for ϕ_l = 80 deg, $R_0 = 2.0X_\sigma$, $\kappa = 2$, $\omega_{y1} = 0.55$, $\omega_{y2} = 0.75$, $\omega_{z1} = 0.7$, and $\omega_{z2} = 0.8$.

a round-nosed waverider. To make the waverider shape more general, the following equation is used:

$$Z = A_1 + B_1 Y^\kappa, \qquad 0 \le Y \le Y_1$$

$$A_1 = \frac{R_0}{\sigma} \tag{21}$$

$$B_1 = \frac{\omega_{z1}}{\omega_{y1}^2}\left(1 - \frac{R_0}{\sigma}\right)\frac{1}{Y_\sigma^2}$$

When $\kappa = 2$, the curve at the nose in the planform plane is a parabola. Different values of κ will produce different waverider nose shapes. The waverider will have smooth freestream and compression surfaces on the symmetry plane when $\kappa > 1$. Figure 7 shows the waverider shape C5 with a rounded nose and a quadrilateral finlet near the base plane in the planform view when $\kappa = 2$, $\omega_{z1} = 0.7$, $\omega_{z2} = 0.8$, $\omega_{y1} = 0.55$, and $\omega_{y2} = 0.75$ for $R_0 = 2.0X_\sigma$ and $\phi_l = 80$ deg. The parabolic nose produces a flatter freestream surface near the symmetry plane and increases the volume. Flatter and wider noses tend to make Δz_{sm} more negative. Thus, the shape with $\kappa = 2$ has a similar static margin as a slender cone even though the finlets are relatively large.

Single Polynomial Planform View

The discontinuities in the planform shapes that are evident in Figs. 4–7 can be eliminated by considering sixth-order even polynomials of the form:

$$Z = Z_0 + AY^2 + BY^4 + CY^6 \tag{22}$$

Three conditions are needed to determine the coefficients A, B, and C in Eq. (22). The first condition is again given by the shock location condition

$$AY_\sigma^2 + BY_\sigma^4 + CY_\sigma^6 = 1 - (R_0/\sigma)$$

To generate a finlet-type structure in the planform plane, two inflection points are required in the range of $0 < Y < Y_\sigma$. For the hexadic polynomial here, these are determined by setting

$$\frac{d^2Z}{dY^2} = 2A + 12BY^2 + 30CY^4 = 0$$

at Y_1 and Y_2, where $0 < Y_1 < Y_2 < Y_\sigma$. When this is done, the coefficients A, B, and C are specified by

$$A = \frac{30\omega_1^2\omega_2^2(\sigma - R_0)}{\sigma[5(\omega_2^2 + \omega_1^2)(6\omega_2^2 - 1) - 2(15\omega_2^4 - 1)]Y_\sigma^2} \tag{23a}$$

$$B = \frac{-5(\omega_2^2 + \omega_1^2)(\sigma - R_0)}{\sigma[5(\omega_2^2 + \omega_1^2)(6\omega_2^2 - 1) - 12(15\omega_2^4 - 1)]Y_\sigma^2} \tag{23b}$$

$$C = \frac{2(\sigma - R_0)}{\sigma[5(\omega_2^2 + \omega_1^2)(6\omega_2^2 - 1) - 2(15\omega_2^4 - 1)]Y_\sigma^2} \tag{23c}$$

where $\omega_1 \equiv Y_1/Y_\sigma$ and $\omega_2 \equiv Y_2/Y_\sigma$. The parameters R_0, ω_1, and ω_2 cannot be selected arbitrarily. The first condition to be imposed is the condition of crossover of the freestream and compression surfaces. It is found that the equivalent noncrossover condition in the planform plane is

$$\left(\frac{dZ}{dY}\right)_{Y=Y_\sigma} \le \left(\frac{Z}{Y}\right)_\sigma \tag{24}$$

By using the relation (24) and Eqs. (23a–23c), the following relation between ω_1 and ω_2 is obtained:

$$\omega_2 \ge \left[\frac{5(3\sigma - 4R_0)\omega_1^2 - 2(5\sigma - 6R_0)}{30(\sigma - 2R_0)\omega_1^2 - 5(3\sigma - 4R_0)}\right]^{1/2} \tag{25}$$

At the nose, $d^2Z/dY^2 = 2A$ when $Y = 0$. For the coordinate system that we use here, the condition $d^2Z/dY^2 > 0$ must hold at the nose. By utilizing inequality (25), the condition $A > 0$ gives

$$\omega_1 > [(6 - \sqrt{21})/15] \approx 0.3074 \tag{26}$$

The maximum value for ω_1 is determined by the condition $\omega_1 = \omega_2$. When the relation (25) is used, the maximum value for ω_1 is given as

$$\omega_1 \le \frac{3\sigma - 4R_0 - \sqrt{(3\sigma - 4R_0)^2 - 12/5(\sigma - 2R_0)(5\sigma - 6R_0)}}{6(\sigma - 2R_0)} \tag{27}$$

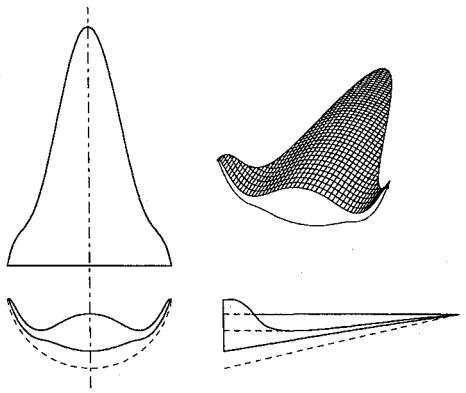

Fig. 8 C6: waverider described by a sixth-order even polynomial leading-edge curve in the planform plane for $\phi_l = 80$ deg, $R_0 = 2.0X_\sigma$, $\omega_1 = 0.39$, and $\omega_2 = 0.82$.

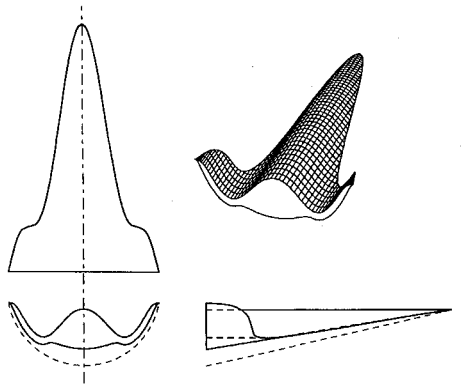

Fig. 9 C7: waverider described by an eighth-order even polynomial leading-edge curve in the planform plane for $\phi_l = 80$ deg, $R_0 = 1.5X_\sigma$, $m = 0.9/Y_\sigma$, $\omega_1 = 0.3$, and $\omega_2 = 0.72$.

For any given R_0, the choice of ω_1 must satisfy the inequalities (26) and (27). When ω_1 is given, the value chosen for ω_2 must satisfy the inequality (25). For $\omega_1 = 0.3074$, the minimum value for ω_2 is found to be 0.7346.

Figure 8 shows the configuration C6 with $\omega_1 = 0.39$ and $\omega_2 = 0.82$ when $R_0 = 2.0X_\sigma$ and $\phi_l = 80$ deg. The sixth-order even polynomial is flexible enough to provide a wide variety of finlets. The static margin for this configuration is not improved as much as might be expected considering the size of the finlets. This is caused by the large dihedral angle of the finlets that contribute little to the longitudinal stability. The vertical finlets, however, may be used for lateral stability purposes. Decreasing ω_2 will increase the size of the finlets, whereas decreasing ω_1 will produce a more dramatic change near the finlet-body intersection.

More terms can be added to the polynomial to increase the flexibility of the planform curve. For the eighth-order even polynomial

$$Z = Z_0 + AY^2 + BY^4 + CY^6 + DY^8 \tag{28}$$

one more condition, $dZ/dY = m$ at $Y = Y_\sigma$, is provided, and the coefficients A, B, C, and D are found to be

$$A = -6\omega_1^2 Y_\sigma^2 B - 15\omega_1^4 Y_\sigma^4 C - 28\omega_1^6 Y_\sigma^6 D$$

$$B = -\frac{5}{2}(\omega_1^2 + \omega_2^2)Y_\sigma^2 C - \frac{14}{3}(\omega_1^4 + \omega_1^2\omega_2^2 + \omega_2^4)Y_\sigma^4 D$$

$$C = \frac{c_1 - b_1 D}{a_1}$$

$$D = \frac{a_1 c_2 - a_2 c_1}{a_1 b_2 - a_2 b_1}$$

where

$$a_1 = \left[\frac{3(1 - 5\omega_1^4)}{(1 - 6\omega_1^2)} - 5(\omega_1^2 + \omega_2^2)\right]\frac{Y_\sigma^2}{2}$$

$$a_2 = \left[\frac{2(1 - 15\omega_1^4)}{(1 - 6\omega_1^2)} - 5(\omega_1^2 + \omega_2^2)\right]\frac{Y_\sigma^2}{2}$$

$$b_1 = \left[\frac{2(1 - 7\omega_1^6)}{(1 - 3\omega_1^2)} - \frac{14}{3}(\omega_1^4 + \omega_1^2\omega_2^2 + \omega_2^4)\right]Y_\sigma^4$$

$$b_2 = \left[\frac{(1 - 28\omega_1^6)}{(1 - 6\omega_1^2)} - \frac{14}{3}(\omega_1^4 + \omega_1^2\omega_2^2 + \omega_2^4)\right]Y_\sigma^4$$

$$c_1 = \frac{m}{4(1 - 3\omega_1^2)Y_\sigma^3}$$

$$c_2 = \frac{\sigma - R_0}{\sigma(1 - 6\omega_1^2)Y_\sigma^4}$$

with the condition $m \leq 1/Y_\sigma$. Figure 9 shows the waverider configuration C7 with $\omega_1 = 0.3$ and $\omega_2 = 0.72$ when $m = 0.9/Y_\sigma$, $R_0 = 1.5X_\sigma$, and $\phi_l = 80$ deg. The eighth-order even polynomial gives more flexibility, and the ranges for ω_1 and ω_2 increase. The finlets for this shape are much larger and wider than those generated by the sixth-order polynomial curve.

Waveriders with Planar Upper-Surface Finlets

It is interesting to consider waveriders that have finlets with flat upper surfaces. This can de done by transferring the planform curve into the base plane, where a straight line is to be fashioned. To this end, $X = F(Y)$ in Eq. (4) is to be specified in the appropriate range. For a finlet with a flat upper surface, $X = F(Y)$ should be a straight line in the base plane, and this can be done by setting

$$F(Y) = (A + BY)\sigma, \quad Y_1 < Y < Y_\sigma \tag{29}$$

such that

$$[f(Y)]^2 = (A + BY)^2 + (1/\sigma^2)Y^2 \tag{30}$$

where the coefficients A and B can be determined by conditions given either in the planform or the base planes. For convenience, these conditions are given by

$$\frac{dX}{dY} = -\tan\Gamma \tag{31}$$

$$Z_1 = f(Y_1) \tag{32}$$

where Γ represents the orientation of the finlets in the base plane, and (Z_1, Y_1) represents the location where the finlets meet the forebody in the planform plane. When Eqs. (31) and (32) are given, the coefficients A and B in Eq. (29) are found to be

$$A = -\sqrt{Z_1^2 - Y_1^2/\sigma^2} + (\tan\Gamma/\sigma)Y_1 \tag{33}$$

$$B = -(\tan\Gamma/\sigma) \tag{34}$$

where $Z_1 = [1 - (R_0/\sigma)]\omega_z + (R_0/\sigma)$ and $Y_1 = \omega_y Y_\sigma$. By substituting Eq. (29) into Eq. (30), the planform leading-edge curve, given by Eq. (3), is therefore given by

$$Z = f(Y) = \left\{\left[\sqrt{Z_1^2 - \frac{Y_1^2}{\sigma^2}} + \frac{\tan\Gamma}{\sigma}(Y_1 - Y)\right]^2 + \frac{Y^2}{\sigma^2}\right\}^{1/2} \tag{35}$$

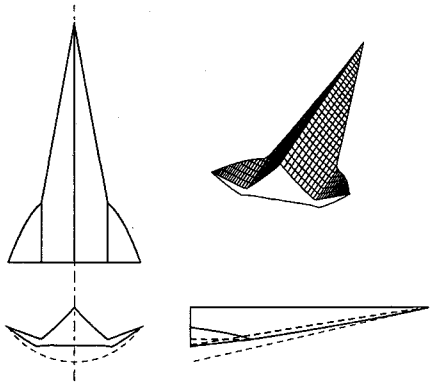

Fig. 10 C8: waverider with planar upper-surface finlets for $R_0 = 0.56X_\sigma$, $\Gamma = -20$ deg, $\omega_y = 0.5$, and $\omega_z = 0.75$.

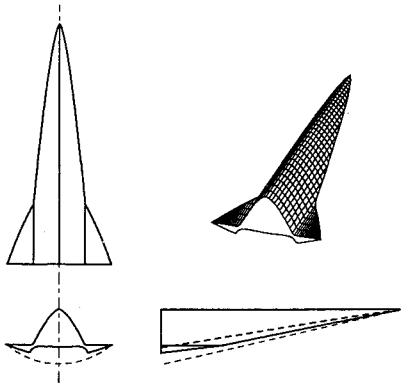

Fig. 11 C9: waverider with planar upper-surface finlets for $R_0 = 0.42X_\sigma$, $\Gamma = 0$ deg, $\kappa = 1.5$, $\omega_y = 0.5$, and $\omega_z = 0.75$.

where the angle Γ is specified. A negative value for Γ represents a finlet reflexed upward. The shock-location condition is no longer an independent condition, it is given by

$$Y_\sigma = \frac{-AB + \sqrt{(AB)^2 - (A^2 - 1)(1/\sigma^2 + B^2)}}{(1/\sigma^2 + B^2)} \tag{36}$$

When Γ, ω_z, and ω_y are specified, the above equation yields a constraint between R_0 and ϕ_l.

Figure 10 shows the waverider shape C8 with $\Gamma = -20$ deg, $\omega_z = 0.75$, and $\omega_y = 0.5$ when $R_0 = 0.56X_\sigma$. This configuration is produced by combining a delta nose and flat upper-surface finlets. The calculated ϕ_l is 55 deg. Figure 11 shows the waverider configuration C9 with $\Gamma = 0$ deg, $\omega_z = 0.75$, and $\omega_y = 0.5$ when $R_0 = 0.42X_\sigma$ and $\kappa = 1.5$. The calculated ϕ_l is 40 deg. The parameter κ is the same as that used for the round-nosed waveriders. The leading-edge curve at the nose is thus a power-law curve with κ as the power. The higher L/D for these two shapes is due to the smaller ϕ_l.

Prescription of Compression Trailing Edge

As a final case, a waverider is considered where the compression trailing edge is specified inboard in the range $0 \le \phi \le \phi_1$, and the freestream trailing edge (for the finlets) is specified outboard in the range $\phi_1 \le \phi \le \phi_l$. This is an alternative to specifying the planform shape in the inboard range, corresponding to Figs. 10 and 11. As an example, a straight-line compression trailing-edge curve is chosen

$$X = R_{b0} = 1 + \omega(\sigma - 1) = \text{const}$$

where $0 < \omega < 1$. The geometry for this case is displayed in Fig. 12.

The inboard freestream trailing-edge curve can be determined as

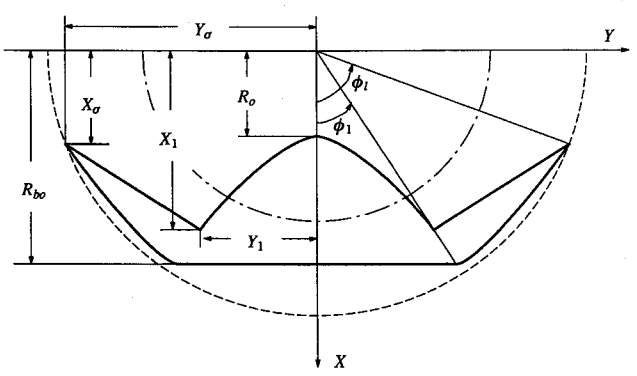

Fig. 12 Notation for combined compression and freestream straight-line trailing edges.

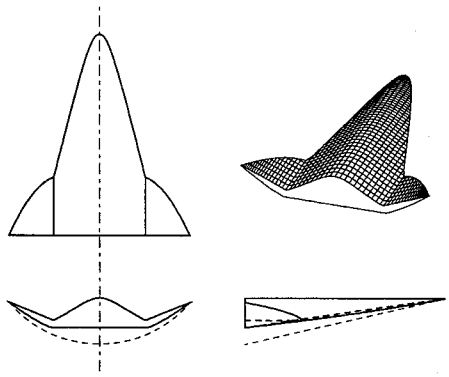

Fig. 13 C10: waverider with planar compression-surface for $\omega = 0.4$, $\phi_1 = 26$ deg, $\phi_l = 50$ deg.

$$X = (1/\sqrt{2})\left[\frac{\sigma^2}{\sigma^2 - 1}(R_{b0}^2 - 1) - Y^2 + \sqrt{Y^4 + \frac{2\sigma^2}{\sigma^2 - 1}(R_{b0}^2 + 1)Y^2 + \frac{\sigma^4}{(\sigma^2 - 1)^2}(R_{b0}^2 - 1)^2}\right]^{1/2} \qquad 0 \le Y \le Y_1 \tag{37}$$

where

$$X_1 = \sqrt{[\sigma^2/(\sigma^2 - 1)](R_{b0}^2 - \cos^2\phi_1)}$$

$$Y_1 = \sqrt{[\sigma^2/(\sigma^2 - 1)](R_{b0}^2 \tan^2\phi_1 - \sin^2\phi_1)}$$

For the finlet, a straight line for the freestream trailing-edge surface is also chosen as

$$X = X_1 + [(X_\sigma - X_1)/(Y_\sigma - Y_1)](Y - Y_1) \qquad Y_1 \le Y \le Y_\sigma \tag{38}$$

Figure 13 shows the resulting waverider configuration C10 for $\omega = 0.4$, $\phi_1 = 26$ deg, and $\phi_l = 50$ deg.

As shown in Table 1, L/D for waveriders with finlets is similar to those without finlets, and varies only slightly while the shapes and locations of the finlets change dramatically. The small variation of L/D is basically affected by ϕ_l. The change of L/D owing to the change of the shape at the same ϕ_l is minimal. The static margins for most waveriders with finlets are less unstable than conventional waverider shapes. Both the size and orientation of the finlets affect the static margin.

Concluding Remarks

An analytical and systematic way of generating waveriders with finlets is presented. Waverider shapes are at first specified by defining a planform leading-edge curve. When this planform curve is varied, different finlet shapes can be obtained and different design requirements can be met. The force and moment coefficients and all the geometric properties of the waveriders are determined by hypersonic small-disturbance theory. For $M_\infty = 8$ and $\delta = 10$ deg, a wide range of example configurations is shown and the aerodynamic and geometric properties are listed and compared. The design procedure is generalized so that the planform shape, free-stream trailing-edge curve, and compression trailing-edge curve can be used separately or in combination to generate a large variety of waverider shapes. The volumetric ratio is only slightly affected because $V^{2/3}$ and S_p decrease at similar rates. The lift-to-drag of waveriders with finlets remains large while the static stability is improved. The theory is readily usable for a variety of design studies.

Acknowledgment

This work was partially supported by Rockwell International under Contract L3GM-408041.

References

[1]Nonweiler, T. R. F., "Delta Wings of Shape Amenable to Exact Shock Wave Theory," *Journal of the Royal Aeronautical Society*, Vol. 67, No. 1, 1963, p. 39.

[2]Jones, J. G., "A Method for Designing Lifting Configurations for High Supersonic Speeds Using the Flow Fields of Nonlifting Cones," Royal Aeronautical Establishment Rept. Aero 2624, Aeronautical Research Council 24846, 1963.

[3]Rasmussen, M. L., "Waverider Configurations Derived from Inclined Circular and Elliptic Cones," *Journal of Spacecraft and Rockets*, Vol. 17, No. 6, 1980, pp. 537–545.

[4]He, X., "Computational Analysis of Hypersonic Flows Past Generalized Cone-Derived Waveriders," Ph.D. Dissertation, School of Aerospace and Mechanical Engineering, Univ. of Oklahoma, Norman, OK, 1992.

[5]Rasmussen, M. L., and He, X., "Analysis of Cone-Derived Waveriders by Hypersonic Small-Disturbance Theory," *Proceedings of the First International Hypersonic Waverider Symposium*, Univ. of Maryland, Dept. of Aerospace Engineering, College Park, MD, 1990, pp. 1–46.

[6]Kim, B. S., Rasmussen, M. L., and Jischke, M. C., "Optimization of Waverider Configurations Generated from Axisymmetric Conical Flows," *Journal of Spacecraft and Rockets*, Vol. 20, No. 5, 1983, pp. 461–469.

[7]Rasmussen, M. L., and Stevens, D. R., "On Waverider Shapes Applied to Aerospace-Plane Forebody Configurations," AIAA Paper 87-2550, Aug. 1987.